Egypt. J. Chem. **Vol. 65**, No. 11 pp. 141 - 154 (2022)

Egyptian Journal of Chemistry

http://ejchem.journals.ekb.eg/

Development of dielectric and magnetic properties of advanced nano-engineering composites

Ali B. Abou Hammad*

Solid State Physics Department, Physics Research Institute, National Research Centre, 33 El Bohouth St., Dokki, Giza 12622, Egypt

Abstract

Highly controlled magnetoelectric, ferroelectric, and nano-engineering composites are promising materials for achieving the requirements of high-performance electronic devices with minimal cost. Thus, multifunctional materials are talented in different applications. In this scope, the properties of nano-engineering materials are mainly related to their macroscopic morphology and microscopic structure. During recent years, there has been a processing interest in synthesis methods and morphology control to give traditional materials innovative functions through the design of the shape, size, porosity, surface, and interface.

Most of the promising concepts of the electrical and magnetic controlling for nanomaterials were based on theoretical assumptions, such as Debye models, which consider the material in the ideal state. The Debye relaxation model was used to explain the relaxation of the dielectric. This model was insufficient in explaining the experimental results, so some modifications were made to explain the experimental results. Cole-Cole model is a modified model to explain the dielectric relaxation with a symmetric broadening in the loss peak. A Cole-Davidson model is a new modification to explain the asymmetric broadening of the loss peak. Havriliak/Negami model is a more comprehensive model and is made to describe both the symmetric and the asymmetric broadening of the loss peak. The dielectric relaxation models are used to describe the dielectric relaxation in the ferroelectric, ferromagnetic, and multiferroic material. The magnetic hysteresis loop is employed to investigate the magnetic order in the composite materials.

Keywords: Dielectric constant; Ferroelectric; Ferromagnetic; magnetoelectric.

1.Introduction

Recently, the miniaturization of devices acquiring great attention to satisfy the requirements of cost reduction and saving space with high performance [1,2]. So, continuous efforts are running on developing information and technology necessary for developing multifunctional materials to fulfil these requirements. The multifunctional materials are widely used in different applications according to their properties; they can be used in the fabrication of various electronic devices and can be used in medical applications depending on the properties of their constituents [3–12].

Multifunctional composites belong to advanced nano-engineering materials. The multifunction composites are fabricated from different constituents with different functions, and they can be fabricated in various forms such as ceramic, powder, thin-film, and membrane according to the desired applications. The fabricated multifunction composites gain the properties of the constituents but with less strength than the individual constituents [13–18]

Polymer-based nanocomposites based on improving the features of the polymer through nanosized filler are a modern class of advanced nano-engineering materials that can be employed in a wide industrial application such as packing, electronics,

*Corresponding author e-mail: abohmad2@yahoo.com.; (Ali B. Abou Hammad).
Receive Date: 31 December 2021; Revise Date: 29 January 2022; Accept Date: 08 March 2022.
DOI: 10.21608/EJCHEM.2022.114030.5184 .

automobile, water treatment, and architecture [19–21]. Nanosized fillers are employed to enhance the different properties of the polymer, such as dielectric strength, processability, durability, rigidness, and flexibility [13,20–25]. Mohd Sadiq et al. 2020 investigated the effect of nanofiller $BaTiO_3$ on the blend PEO-PVC polymer electrolyte with $LiClO_4$. They found that ionic conductivity and dielectric constant were increased with the insertion of the nanofiller $BaTiO_3$ into the polymer matrix. They attributed the enhancement in ionic conductivity and dielectric constant to disrupting the crystalline arrangement by the incorporation of the nanofiller into the polymer chain. Therefore, they referred to the possibility to use this polymer matrix as a solid polymer electrolyte in the energy storage devices [26].

The different materials are classified into diamagnetic materials, paramagnetic materials, and ferromagnetic materials according to their response to the external magnetic field. The magnetic properties depend on the spin motion of single electrons in the d-orbital. The first class is the diamagnetic material where it shows a negative response to the applied magnetic field [27–29]. The second class is the paramagnetic material, where it shows a positive response to the applied magnetic field and doesn't maintain the magnetism after removing the applied magnetic field [27–29]. The third class is the ferromagnetic material, which shows a positive response to the applied magnetic field and maintains the magnetization after removing the applied magnetic field, Fig.1 Therefore, a demagnetizing field is applied in the reverse direction to remove the remanent magnetization [9,14,30].

Ferrites nanoparticles (MFe_2O_4; M= Fe, Co, Ni, Mn, & Zn) with the spinel structure AB_2O_4 belong to the ferromagnetic class and they gain great attention due to their enormous applications in various fields such as biomedical and industrial applications [15,31–34]. Ferrites NPs can be used for drug delivery, tumor treatment [35,36], controlled drug release, tissue repair [37] and magnetic resonance imaging [38]. Also, Ferrites NPs can be used as adsorbents, catalysts [39,40], wastewater treatment [15], sensors, and biosensors [41].

On the other hand, the response of the materials to the surrounded external electric field determines the type of the materials, where the different materials can be classified as ferroelectric and non-ferroelectric. The external electric field induces electric polarization in the non-ferroelectric materials, which will be vanished with removing the external electric field. On the contrary, the ferroelectric material maintains the polarization (spontaneous polarization) after removing the external electric field. Ferroelectric NPs behave like ferromagnetic NPs and they need a depolarizing field in the reverse direction to remove the remanent polarization [42,43].

Ferroelectric material with a perovskite structure (ABO_3: A is Ba, Sr, Pb, Mn, Mg…. and B is Zr, Ti, Fe, Sn …) is the most interesting ferroelectric material [8,17,44]. The ferroelectric material is characterized by an offset between the different charge centers, and it undergoes a transition from centrosymmetric to noncentrosymmetric at the Curie temperature [45,46].

Another interesting multifunctional material is the advanced nano-engineering magneto-electric composite. Researchers are making strenuous attempts to produce advanced multifunctional nano-engineering materials with high permeability and permittivity [47]. Advanced magneto-electric compounds belong to the advanced nano-engineering composites that are characterized by their magneto-electric effect, where they are polarized when exposed to a magnetic field (H) and magnetized when exposed to an electric field (E) [48]. Therefore, such compounds should contain both electric and magnetic dipoles. They are founded in composites that contain both ferroelectric and ferromagnetic constituents. These materials were first suggested by Van Suchetelene [48,49]. This new class of materials is characterized by its advanced properties and the co-existence of ferromagnetic and ferroelectric orders, Fig.1. The magneto-electric effect can exist in single-phase ($BiFeO_3$) or multi phases composite ($BaTiO_3/CoFe_2O_4$).

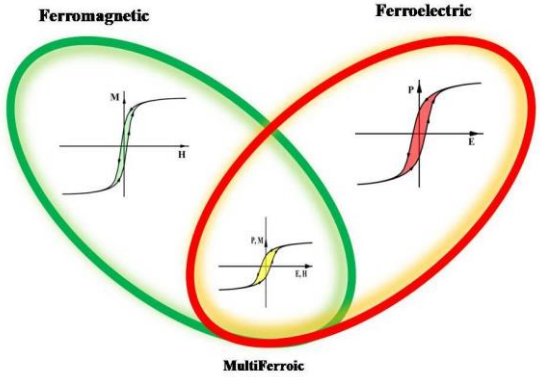

Fig.1, Schematic representations of Ferromagnetic, Ferroelectric, and Multiferroic.

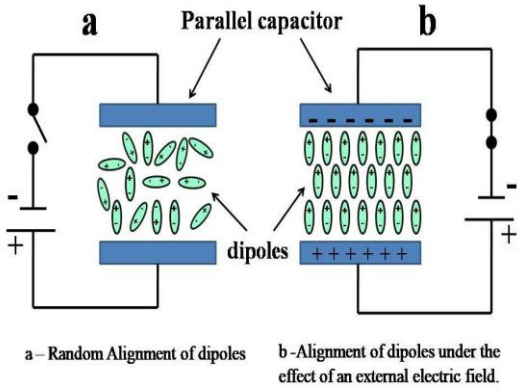

Fig.2 parallel plates capacitor.

2. Dielectrics

Studying the dielectric relaxation in solid is a highly interesting topic in modern physics. Dielectric Relaxation is related to the motion of the dipoles inside materials. Moreover, the dielectric response of materials is affected by the drift motion of the mobile charge carriers such as vacancies, ions, electrons, and charged defects because they increase the conductivity contributions to the dielectric response [50,51].

2.1. Dielectric polarization

The dielectric polarization occurs when a dielectric material is introduced between two parallel electrodes connected to an external electric field, where the charge carriers undergo a motion towards the oppositely charged electrode under the effect of the external field. There are different types of polarization that occur inside materials. The type of polarization depends on the nature of the materials. The first type of polarization is known as orientational polarization. The orientational polarization occurs inside materials that have permanent dipoles but are randomly oriented in absence of external fields [13,25]. The second type of polarization is induced polarization; it occurs inside materials that haven't permanent dipoles and a displacement occur between opposite charges under the influence of an external field. The other types of polarization are electrode polarization, interfacial polarization, ionic polarization, and electronic polarization [13,23,25]. Fig.2 shows the effect of the applied electric field on the different dipoles inside the material between the parallel plates capacitor.

2.2. Dielectric constant (Permittivity)

2.2.1. Dielectric constant in static electric field

Fig.2b shows the alignment of the different dipoles inside the substance under the effect of static external electric field. The polarization of substance (P) is given by the number of dipoles per unit volume of the substance. The polarization of substance is proportional to the external electric field (E); it given by

$$P = \varepsilon_0 \chi E \ldots\ldots\ldots\ldots\ldots \quad (1)$$

where χ is the electric susceptibility and ε_0 is the free space permittivity (ε_0 = 8.854 * 10^{-12} F/m). The electrical displacement D is correlated with the polarization P through the following equation:

$$D = \varepsilon_0 E + P \ldots\ldots\ldots\ldots\ldots \quad (2)$$

From equation no 1 and 2

$$D = \varepsilon_0 E + \varepsilon_0 \chi E = \varepsilon_0 (1 + \chi) E \ldots\ldots\ldots\ldots\ldots \quad (3)$$

$$D = \varepsilon E = \varepsilon_0 \varepsilon_r E \ldots\ldots\ldots\ldots\ldots \quad (4)$$

$$\varepsilon = \varepsilon_0 \varepsilon_r \ldots\ldots\ldots\ldots\ldots \quad (5)$$

ε is the permittivity of the material and ε_r the relative permittivity of substance, it given by

$$\varepsilon_r = \frac{\varepsilon}{\varepsilon_0} = 1 + \chi \ldots\ldots\ldots\ldots\ldots \quad (6)$$

The relative permittivity of material is known as the dielectric constant of the material [51,52].

2.2.2. Dielectric constant in alternating electric field.

Applying an alternating electric field on the parallel plate's capacitor leads to frequent changes in the polarity of the electrode capacitor. Therefore, the direction of the dipoles of the material will follow the polarity change of the electrodes.

The field is given by

$$E(t) = E_0 \, e^{i\omega t} \ldots\ldots\ldots\ldots\ldots \quad (7)$$

where E(t) is time dependent field, ω is the angular frequency ($2\pi f$) and f is the field frequency. Thus, the polarization of the substance in an alternating field will be lag behind the external field and can't keep in change with the field, and so the electrical susceptibility is given by

$$\chi(\omega) = \chi'(\omega) - i\chi''(\omega) \quad \text{..... (8)}$$

χ' and χ″ are the real and the imaginary part of the electrical susceptibility. Therefore, according to equation no.5, the relative permittivity of the substance will be a complex quantity and it becomes;

$$\varepsilon^*(\omega) = \varepsilon'(\omega) - i\varepsilon''(\omega) \quad \text{..... (9)}$$

The real part of the relative permittivity ε′(ω) gives the dielectric constant of the substance as a function of the frequency of the applied field, while the imaginary part ε″(ω) defines the dielectric loss of the substance as a function of frequency. The dielectric constant and the dielectric loss have a long-range spectrum over a wide range of frequencies from 1μHz to 10^{15} Hz. The behaviour of the dielectric constant and the dielectric loss over this wide range of frequencies depends on the different polarization mechanisms that occur inside the dielectric material [53].

The spectrum of the dielectric constant and the dielectric loss with the different polarization mechanisms that occur inside the different materials over the frequency of the applied field is presented in Fig.3.

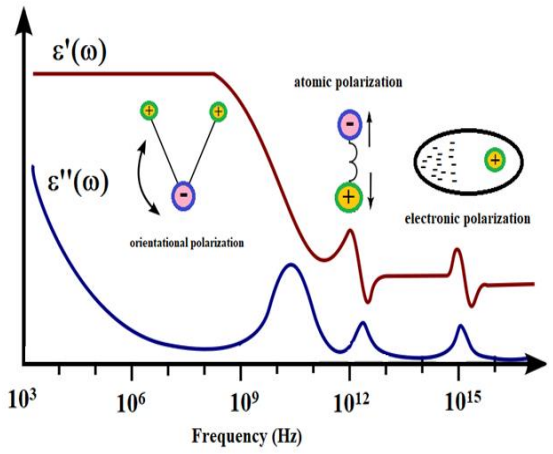

Fig.3. the different polarization mechanisms versus the frequency of the applied field.

The permittivity (ε) of the material between the two parallel electrodes is related to the capacitance (C) through the following relation

$$\varepsilon = C\,\frac{t}{A} \quad \text{..... (10)}$$

where t is the thickness of the material and A is the area of the electrode.

From equations no. (6 and 10) the relative permittivity (dielectric constant) of the material is given by

$$\varepsilon_r = \frac{\varepsilon}{\varepsilon_0} = \frac{C\,t}{\varepsilon_0\,A} \quad \text{..... (11)}$$

Equation number 11 is used to calculate the dielectric constant experimentally.

2.3. Dielectric relaxation

Applying an alternating electric field on the parallel plate's capacitor leads to frequent changes in the polarity of the electrode capacitor. Thus, the permittivity of the material between the parallel plates is frequency dependent eq.9;

$$\varepsilon^*(\omega) = \varepsilon'(\omega) - i\,\varepsilon''(\omega)$$

where ε*(ω) is a complex permittivity function, ε ′(ω) represents the dielectric constant and it proportional to the energy stored in the material, and the imaginary part ε ″(ω) represents the dielectric loss and it proportional to the dissipated energy. The experimental dielectric measurements are usually analysed though different relaxation models. Several models are suggested to interpreting the experimental dielectric spectrum starting from the theoretical Debye model. These models gave information about the mechanism of the molecular dynamics inside the materials under the effect of the external electric field.

Neagu et al [54]studied the dielectric relaxation of chitosan film loaded with $BaTiO_3$ nanoparticles at room temperature. They attributed the high dielectric constant at low frequency to the interfacial polarization and electrode polarization. While the dielectric constant that released from the intrinsic properties of the materials appeared at the frequency above 1kHz. The loss peak of the composite samples was appeared also around 1 kHz which is associated to α-relaxation in chitosan matrix [54].

2.3.1. Debye Relaxation

The Debye relaxation neglects the inertia effects and considers the ideal conditions in interpretation the complex permittivity ε*(ω) behaviour with the sweeping frequency of the applied external field E(ω) [55,56].

The complex permittivity of the material is given by

$$\varepsilon^*(\omega) = \varepsilon_\infty + \frac{\Delta\varepsilon}{1+i\omega\tau_D} \quad \ldots\ldots\ldots\ldots\ldots \quad (12)$$

$\Delta\varepsilon$ is the dielectric strength and it given by

$$\Delta\varepsilon = \varepsilon_S - \varepsilon_\infty \quad \ldots\ldots\ldots\ldots\ldots \quad (13)$$

Therefore, the real and imaginary parts of the complex permittivity are given by

$$\varepsilon'(\omega) = \varepsilon_\infty + \frac{\varepsilon_S - \varepsilon_\infty}{1+(\omega\tau_D)^2} \quad \ldots\ldots\ldots\ldots\ldots \quad (14)$$

$$\varepsilon''(\omega) = \frac{(\varepsilon_S - \varepsilon_\infty)\omega\tau_D}{1+(\omega\tau_D)^2} \quad \ldots\ldots\ldots\ldots\ldots \quad (15)$$

ε_S is the dielectric permittivity at the low frequency nearly zero frequency, while ε_∞ is the dielectric permittivity at the high frequency. τ_D is the Debye relaxation time [55,56]. Figure 4 shows the behavior of the real and imaginary parts of the dielectric permittivity according to the theoretical Debye model. The real dielectric permittivity $\varepsilon'(\omega)$ shows a step-like decrease which is used to calculate the dielectric strength $\Delta\varepsilon$ as indicated in the figure, Fig.4. While the imaginary dielectric permittivity $\varepsilon''(\omega)$ shows a peak with symmetric broadening. The peak frequency (ν_p) is used to calculate the relaxation time (τ_p), where $\tau_p = 1/\omega_p = 1/(2\pi\nu_p)$[56].

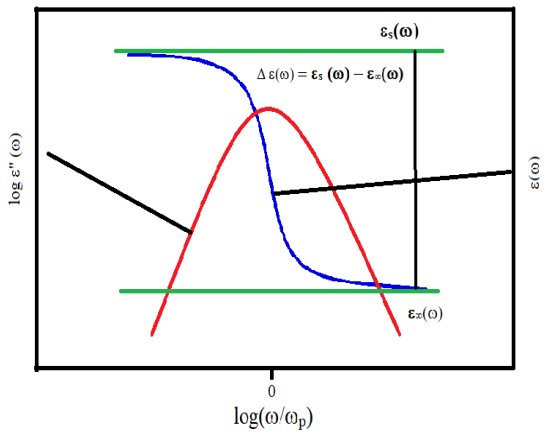

Fig.4 Real ε' and imaginary part ε'' of the complex dielectric function vs normalized frequency for a Debye relaxation process.

2.3.2. Non-Debye relaxation

The Debye relaxation behaviour is rarely observed, while the dielectric measurements in many cases are much broader and in other cases are asymmetric. This behaviour is known as a non-Debye relaxation. In such cases, the spectrum of the dielectric measurements arises from the distribution of different environments (defects, free charge carriers, space charge….etc). Therefore, several empirical models, which are generalized of the Debye model, have been improved to be able to interpret the asymmetric and/or broadened in the loss peaks [57].

Cole K. and Cole R. (1941) suggested a modification on the Debye model to describe the broadening in the loss peak [58].

$$\varepsilon^*(\omega) = \varepsilon_\infty + \frac{\Delta\varepsilon}{1+(i\omega\tau_{CC})^\beta} \quad \ldots\ldots\ldots\ldots\ldots \quad (16)$$

This model is known as Cole/Cole model in which $0 < \beta \leq 1$which describes the broadening of the loss peaks. This model reduced to Debye model when $\beta = 1$.

Davidson D. and Cole R. (1950) suggested another modification to the Debye model to describe the asymmetric broadening of the loss peaks, this model is known as Cole/Davidson [59,60].

$$\varepsilon^*(\omega) = \varepsilon_\infty + \frac{\Delta\varepsilon}{(1+i\omega\tau_{CD})^\gamma} \quad \ldots\ldots\ldots\ldots\ldots \quad (17)$$

Where $0 < \gamma \leq 1$ and it describes the asymmetric broadening of the loss peaks.

Havriliak and Negami (1966) introduced a more general formula that combines these three models [57];

$$\varepsilon^*_{HN} = \varepsilon_\infty + \frac{\Delta\varepsilon}{(1+(i\omega\tau_{HN})^\beta)^\gamma} \quad \ldots\ldots\ldots\ldots\ldots \quad (18)$$

β and γ ($0 < \beta;\beta\gamma \leq 1$) are the fractional shape parameters and they describe the broadening, the symmetric, and the asymmetric broadening of the complex dielectric measurements [61].

Deka et al [62] studied the dielectric properties of $Bi_{1-x}Sm_xFeO_3$ (with x = 0, 0.1, 0.2 and 0.3). They attributed the sharp fall of the relative permittivity after the observed plateau at low frequency to the relaxation mechanism of the internal dipoles and this relaxation was confirmed by the peaks in the dielectric loss. They used the modified Havriliak/Negami equation to interpret their data;

$$\varepsilon^*_{HN} = \varepsilon_\infty + \frac{\Delta\varepsilon}{(1+(i\omega\tau_{HN})^\beta)^\gamma} - i\frac{\sigma^*}{\varepsilon_0\omega^s} \quad \ldots\ldots\ldots \quad (19)$$

where σ^* represents the conductivity contribution to the permittivity and it given by $\sigma^* = \sigma' + j\sigma''$. Here σ' is assigned to the conductivity released from the free charge carriers, while σ'' is assigned to space charges (localized charges).

2.3.3. Electric modulus

The complex electric modulus $M^*(\omega)$ is used for the interpretation of experimental data instead of the complex dielectric permittivity. The Electric Modulus spectroscopy was suggested for the first time in 1967 [63,64]. The electric modulus is meaningful when the capacitance of the substance is composed of different capacitive elements Which results in a difference in relaxation times [65]. Thus, it is a useful method for

defining the teeny contribution of the capacitance in the substances [66]. Also, it is a powerful method to define the mechanism of the charge transport, conduction process, and the dielectric relaxation [64,67,68].

$$M^*(\omega) = M'(\omega) + i\,M''(\omega) \quad \text{..... (20)}$$

$$M^*(\omega) = \frac{1}{\varepsilon^*(\omega)} = \frac{\varepsilon'(\omega)+i\,\varepsilon''(\omega)}{\varepsilon'^2(\omega)+\varepsilon''^2(\omega)} \quad \text{..... (21)}$$

Therefore,

$$M'(\omega) = \frac{\varepsilon'(\omega)}{\varepsilon'^2(\omega)+\varepsilon''^2(\omega)} \quad \text{..... (22)}$$

$$M^*(\omega) = \frac{1}{\varepsilon^*(\omega)} = \frac{i\,\varepsilon''(\omega)}{\varepsilon'^2(\omega)+\varepsilon''^2(\omega)} \quad \text{..... (23)}$$

Mumtaz et al [64] used the complex electric modulus to define and analyse the different dynamical mechanism of electric transport in $MnFe_2O_4/Cu_{0.5}Tl_{0.5}Ba_2Ca_2Cu_3O_{10-\delta}$(CuTl-1223). Also, they used the complex electric modulus to differentiate between the effects of grain and grain-boundaries on the electrical properties of the composite. They attributed the very tiny value of the real electric modulus M′(ω) of the composite at the low frequency to the effect of the electrode polarization is neglected. Also, they attributed the saturation at the high frequency to the short-range hopping of the charge carriers. They investigated that the frequency of the peak of the imaginary electric modulus separates between the long-range hopping at low frequency and the short-range hopping at high frequency.

2.4. Ferroelectricity and ferroelectric materials

Ferroelectric materials belong to the most important dielectric materials. Ferroelectricity and Ferroelectric materials describe the materials that have permanent dipoles which are spontaneously polarized and adjust their position through orientation with the external electric field. Thus, a ferroelectric hysteresis loop describes the relation between the external electric field (E) and the polarization (P) of the material [69,70] Fig.5.

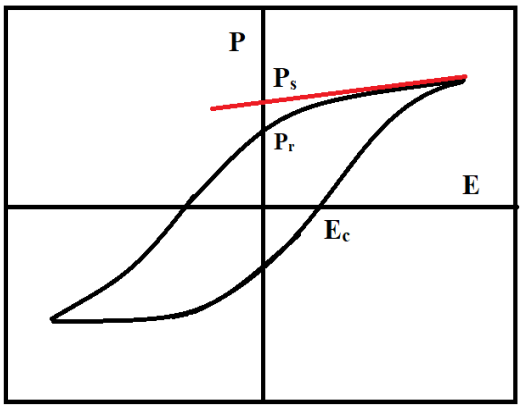

Fig. 5 the relation between the electric polarization (P) and the driving electric field (E). P_s describes the spontaneous polarization, P_r, describes the remanent polarization at zero electric field, and the E_c describes the coercive field which is required to reduce the polarization to zero.

Ferroelectric materials are widely used due their amazing properties. It can be used in fabrication of multilayer ceramic capacitors, supercapacitors, resistors, transducers, actuators….etc [71]. Ferroelectric ceramic such as Barium Titanate ($BaTiO_3$) is characterized by its high dielectric constant. The ferroelectric materials are characterized by the phase transition at a Curie temperature T_C, where the ferroelectric materials are transformed from the polar state under the Curie temperature to the unpolar state above the Curie temperature. The dielectric constant of the ferroelectric materials reaches a high value at the Curie temperature and fastly decreases above the transition temperature. Thus, the dielectric constant of the ferroelectric materials obeys the Curie Weiss low above the transition point (T_C) [71];

$$\varepsilon'(\omega) = \frac{C}{T-T_C} \quad \text{..... (24)}$$

C is the Curie constant [72].

Yuan et al [73] fabricated a ferroelectric $(Ba_{1-x}Cd_x)TiO_3$ ($0 \le x \le 0.25$) ceramics by a conventional solid-state method and investigated the effect of Cd^{2+} concentration on the dielectric properties and the phase transition of the ferroelectric $BaTiO_3$. They investigated that the electrical and the ferroelectric properties were optimized for $Ba_{0.95}Cd_{0.05}TiO_3$.

Wei et al [74] synthesized a free lead ferroelectric ceramic $[(Ba_{0.85}Ca_{0.15})_{1-3x/2}Bi_x](Zr_{0.1}Ti_{0.9})O_3$ (BCZT-Bi). They investigated that addition of Bi^{3+} ions into BCZT decreases the maximum of the dielectric constant at the transition temperature and increase the

broadening of the peaks. They demonstrated that the dielectric constant of their materials obeys the modified Curie Weiss low;

$$\frac{1}{\varepsilon'} - \frac{1}{\varepsilon'_m} = \frac{(T-T_m)^\gamma}{C} \quad \text{..... (25)}$$

where ε'_m is the maximum dielectric constant at the transition temperature, while γ describes the diffused phase transition, ($1 \le \gamma \le 2$). When γ equal to unity it describes the classical ferroelectric materials, while $\gamma = 2$ it describes the relaxor ferroelectric materials. They found that the transition temperature decreased from 94 ^oC to 5 ^oC as the Bi^{3+} increased and the defused coefficient γ increased. They attributed this behavior to the replacement of $(Ba,Ca)^{2+}$ ions by the Bi^{3+} destroy the long rang ferroelectric order at the A-site. They concluded that ceramics contain Bi^{3+} ions show a strong relaxor ferroelectric behavior [74].

Zhang et al [71] studied the effect of Sc_2O_3 on the ferroelectric properties of $Ba(Zr_{0.1}Ti_{0.9})O_3$, (BZT). They investigated that BZT doped scandium oxide had a perovskite structure with a tetragonal phase and the grain size reduced from 40 μm to nearly 5 μm. They investigated that all samples have a ferroelectric - paraelectric transition temperature T_C and the transition temperature moved to a low temperature with increasing the scandium concentration.

They attributed this behaviour to a presence of a diffused phase transition that resulted from the disorder arrangement in the A and B site cations. Also, this disorder results in a decrease in the spontaneous polarization of the samples.

3. Magnetism

Magnets have a definitive role in modern life, where a huge number of devices are utilized in the industry based on the electromagnetic. The magnetic phenomena were discovered in ancient times where humans discovered the magnetization in natural minerals such as iron and magnetite. The magnetic phenomena were not appreciated based on the electromagnetic theory until Faraday and Oersted introduced their theory. Materials are categorized based on their response to the external magnetic field into three groups, ferromagnetic, paramagnetic, and diamagnetic. The response of the materials to the external magnetic field is determined from the relation between the magnetization (M) and the applied magnetic field (H) [75].

$$M = \chi_m H \text{ ..... (26)}$$

χ_m is the magnetic susceptibility.

Figure 6 shows the relations between the magnetization (M) and the driving magnetic field (H) for the three main groups of the material [76]. The ferromagnetic materials are known as magnetic materials and they are singular due to their ability to transfer force and energy through intervening substances without contacts or wires [76].

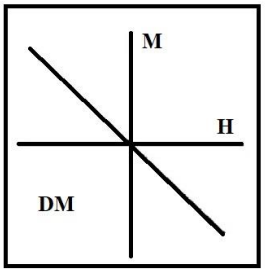

a- Negative response of diamagnetic material to the driving magnetic field.

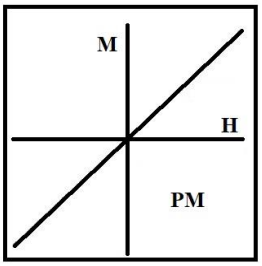

b- Positive response of paramagnetic material to the driving magnetic field.

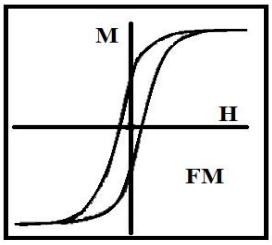

c- A positive response with hysteresis loop of the ferromagnetic material to the driving magnetic field.

Fig.6 the magnetic response of the different materials to the driving magnetic field.

3.1. Spinel Magnetic materials

Ferrite nanoparticles with spinel structure are a class of the most amazing magnetic nanoparticles. The spinel ferrites gained intensive research in the last years because of their interesting physical properties, which candidate them in various applications such as magnetic recording, electric motors, sensors, transformers, biomedicine, and water treatment [77]. The conceivable applications of the spinel magnetic nanoparticle depend on the magnetic properties of the materials such as saturation magnetization, coercivity, remanent magnetization, and the blocking temperature. The spinel ferrite has a cation distribution between the octahedral site and the tetrahedral sites that affect the magnetic properties of the ferrite [77,78]. The spinel ferrite has the general formula MFe_2O_4 (where M

represents a divalent ion such as Fe, Co, Mg, Zn, Mn, Ni). Spinel ferrites belong to the magnetic ceramic materials in which the oxygen ions occupy the close-packed face-centred cubic structure. While the M^{2+} ions occupy the tetrahedral sites and the Fe^{3+} ions occupy the octahedral sites in the normal spinel ferrite. In the inverse spinel structure, the Fe^{3+} ions occupy both the octahedral and the tetrahedral sites while the M^{2+} ions occupy part of the octahedral sites, Fig.7. Also, there is a partial inverse spinel structure in which the cations M^{2+} and Fe^{3+} occupy both the octahedral and the tetrahedral sites. $ZnFe_2O_4$ is an example of the normal spinel structure where Zn^{2+} occupies the tetrahedral while Fe^{3+} occupies the octahedral sites. While, $CoFe_2O_4$ and $NiFe_2O_4$ are examples of the inverse spinel structure, in which the divalent ions Co^{2+} and Ni^{2+} occupy half of the octahedral sites with half of the Fe^{3+} ions while the other half of the Fe^{3+} ions occupy the tetrahedral sites [78–80].

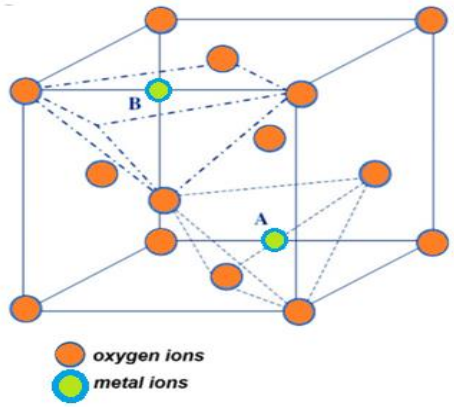

Fig.7 the crystal structure of the spinel ferrite

The magnetic properties of the spinel ferrite are affected by the preparation methods, the starting precursors, the heat treatment, and the particle size.

Sepelak et al [81] investigated the effect of annealing temperature on the magnetic properties of the milled $NiFe_2O_4$. They attributed the enhancements of the properties to the re-equilibration distribution of the cations and the disappearance of the canted spin.

Reddy and Yun [82] reported that spinel ferrites with the general formula MFe_2O_4 possess unique physicochemical properties such as high chemical stability, active sites, high specific surface area, tunability, and excellent magnetic properties. They reported that such magnetic materials are good adsorbents for water purification especially for waters that require adsorbents with rapid kinetics and high adsorption efficiency and it can be easily removed from the aqueous solution through magnets.

Magnetic materials are widely spread in industrial applications. The magnetic nanoparticles can be used in the fabrication of different motors, the aviation industry, motors for household equipment, transformers, inductors, and telecommunications equipment. Also, it can be used in the medicine application such as separation of cancer cell, drug delivery, and fabrication of magnetic resonance devices [83].

3.2. Magnetic measurement technique

The most important technique that is used to record the magnetic moment and magnetization of the materials is the Vibrating Sample Magnetometry (VSM). EZ9-HF High Field vector vibrating sample magnetometer (VSM) is used for measuring the magnetic anisotropy and magnetization over a wide range of temperature. Also, the VSM device is used to determine the magnetic hysteresis loop and the magnetic properties of the samples with a different forms, thin films, powders, and bulk.

The VSM works by inserting the sample in a perpendicular way to the magnetizing field. This technique can detect the small change in the magnetic moment and magnetization in the range 10^{-5} to 10^{-6} emu. This technique based on the magnetic sample is attached to the sample holder which is inserted between two working electromagnetic poles. The sample is placed in a position known as saddle point, which is obtained through calibration before measurements. A constant vibration with a fixed frequency (ω) is exerted on the sample during measurement [84].

4. Multiferroic

Multiferroic materials are an interesting multifunctional material. Multiferroic nanoarticles refer to the materials that combine between at least two of the ferroic properties such as ferroelectric, ferromagnetic, ferrofluid, antiferromagnetic, etc. Multiferroic nanoparticles that combine between the ferroelectric and ferromagnetic materials exhibit coupling between electric and magnetic fields. They become magnetized when placed in electric field and get polarized when placed in magnetic field [85].

Yang et al [86] prepared multiferroic BNT-CFO ($Bi_{3.15}Nd_{0.85}Ti_3O_{12}$–$CoFe_2O_4$) thin film by spin-

coating on Pt/Ti/SiO2/Si substrate. Where they prepared the first layer BNT on the substrate then they added the second layer CFO to the first layer. They investigated the ferroelectric hysteresis loop of the BNT-Film which proves the presence of the ferroelectricity in the composite film. Also, they prove the presence of the ferromagnetic order in the composites. Thus, the composite film combines between the ferroelectric and the ferromagnetic order, therefore the composite film is a multiferroic film [86].

Multiferroic materials are highly interdisciplinary and cover a wide range of objects and technologies including energy harvesting, data storage, random access memories, recording technologies, microwave devices, sensors, photovoltaic technologies, and solid-state refrigeration. it is expected that multiferroic materials could reach up to multibillion US dollars in market value [87].

5. Conclusion

The rapid development of industrial technology in different fields requires understanding the motion mechanism of the charging carriers inside materials. Therefore, it stimulated the scientists to develop their dielectric and magnetic theories to fulfil the required technology and understand the material's behaviour under the external effects. The dielectric models such as Cole-Cole, Cole-Davidson, and Havriliak-Negami identify the relaxation mechanism of the dielectric materials, where Cole-Cole and Cole-Davidson are used for the interpretation of the symmetric and the asymmetric broadening of the peak of the dielectric loss $\varepsilon''(\omega)$, respectively, while the Havriliak-Negami model is useful for the interpretation of the mixed relaxation process. Also, the magnetic properties of nanoparticle and composite materials play a significant role in identifying the application of the materials. The dielectric and magnetic materials are extensively used in the fabrication of devices in different fields including the electronic and medical industry. Therefore, scientists are working on developing electrical and magnetic materials and developing their electromagnetic properties to expand their various applications. Ferroelectric, ferromagnetic, and multiferroic materials belong to the most important materials that have been developed recently due to the wide scope of their application in electronic, medical, industrial, and communication applications. Multiferroic materials gain special attention from scientists due to their multi-functionality and their possibility to perform many tasks simultaneously. Recently, scientists seeking advanced multiferroic materials with comparable properties to the properties of the ferroelectric and ferromagnetic. Furthermore, developing new models to understand the dynamical motion of the charge carriers and spin motion of the electrons to expand their applications.

6. Reference

[1] H. Su, X. Tang, H. Zhang, Y. Jing, F. Bai, Low-Loss Magneto-Dielectric Materials: Approaches and Developments, Journal of Electronic Materials. 43 (2014) 299–307. https://doi.org/10.1007/s11664-013-2831-5.

[2] B. Xiao, Y. Dong, N. Ma, P. Du, Formation of Sol-Gel In Situ Derived BTO/NZFO Composite Ceramics with Considerable Dielectric and Magnetic Properties, Journal of the American Ceramic Society. 96 (2013) 1240–1247. https://doi.org/10.1111/jace.12181.

[3] M.A. Moharram, K.M.T. Ereiba, W. El Hotaby, A.M. Bakr, Synthesis and characterization of graphene oxide/crosslinked chitosan nanaocomposite for lead removal form aqueous solution, Research Journal of Pharmaceutical, Biological and Chemical Sciences. 6 (2015) 1473–1489.

[4] A.A. Al-esnawy, K.T. Ereiba, A.M. Bakr, A.S. Abdraboh, Characterization and antibacterial activity of Streptomycin Sulfate loaded Bioglass/Chitosan beads for bone tissue engineering, Journal of Molecular Structure. 1227 (2021) 129715. https://doi.org/10.1016/j.molstruc.2020.129715.

[5] W. El hotaby, A.M. Bakr, H.S. Ibrahim, N.S. Ammar, H.A. Hani, A.A. Mostafa, Eco-friendly zeolite/alginate microspheres for Ni ions removal from aqueous solution: Kinetic and isotherm study, Journal of Molecular Structure. 1241 (2021) 130605. https://doi.org/10.1016/j.molstruc.2021.130605.

[6] A. Bakr, B. Anis, W. El hotaby, Sounchemical synthesis of Graphene/nano hydroxyapatite composites for potential biomedical application, Egyptian Journal of Chemistry. 65 (2021) 0–0. https://doi.org/10.21608/ejchem.2021.91241.4339.

[7] Y. Peng, X. Wu, Z. Chen, W. Liu, F. Wang, X. Wang, Z. Feng, Y. Chen, V.G. Harris, BiFeO3 tailored low loss M-type hexaferrite composites having equivalent permeability

and permittivity for very high frequency applications, Journal of Alloys and Compounds. 630 (2015) 48–53. https://doi.org/10.1016/j.jallcom.2015.01.026.

[8] A.M.E. el Nahrawy, A.M. Bakr, A.B.A.A. Hammad, B.A. Hemdan, High performance of talented copper/magneso-zinc titanate nanostructures as biocidal agents for inactivation of pathogens during wastewater disinfection, Applied Nanoscience. 10 (2020) 3585–3601. https://doi.org/10.1007/s13204-020-01454-3.

[9] A.B. Abou Hammad, M.E. Abd El-Aziz, M.S. Hasanin, S. Kamel, A novel electromagnetic biodegradable nanocomposite based on cellulose, polyaniline, and cobalt ferrite nanoparticles, Carbohydrate Polymers. 216 (2019) 54–62. https://doi.org/10.1016/j.carbpol.2019.03.038.

[10] A.B. Abou Hammad, A.G. Darwish, A.M. El Nahrawy, Identification of dielectric and magnetic properties of core shell ZnTiO3/CoFe2O4 nanocomposites, Applied Physics A. 126 (2020) 504. https://doi.org/10.1007/s00339-020-03679-z.

[11] M.M. Elokr, F. Metawe, A.M. El-Nahrawy, B.A.A.A. Osman, A.M. El Nahrawy, B.A.A.A. Osman, Enhanced structural and spectroscopic properties of phosphosilicate nanostructures by doping with Al2O3 ions and calcinations temperature, International Journal of ChemTech Research. 9 (2016) 228–234.

[12] A.M. ElNahrawy, A.B. AbouHammad, A facile co-gelation sol gel route to synthesize cao: P2o5: Sio2 xerogel embedded in chitosan nanocomposite for bioapplications, International Journal of PharmTech Research. 9 (2016) 16–21.

[13] A.M. El-Nahrawy, A.B. Abou Hammad, T.A. Khattab, A. Haroun, S. Kamel, Development of electrically conductive nanocomposites from cellulose nanowhiskers, polypyrrole and silver nanoparticles assisted with Nickel(III) oxide nanoparticles, Reactive and Functional Polymers. 149 (2020) 104533. https://doi.org/10.1016/j.reactfunctpolym.2020.104533.

[14] A.M. el Nahrawy, A. Elzwawy, A.B. Abou Hammad, A.M. Mansour, Influence of NiO on structural, optical, and magnetic properties of Al2O3–P2O5–Na2O magnetic porous nanocomposites nucleated by SiO2, Solid State Sciences. 108 (2020) 106454. https://doi.org/10.1016/j.solidstatesciences.2020.106454.

[15] A.B. Abou Hammad, B.A. Hemdan, A.M. el Nahrawy, Facile synthesis and potential application of Ni0.6Zn0.4Fe2O4 and Ni0.6Zn0.2Ce0.2Fe2O4 magnetic nanocubes as a new strategy in sewage treatment, Journal of Environmental Management. 270 (2020) 110816. https://doi.org/10.1016/j.jenvman.2020.110816.

[16] A.M. el Nahrawy, A.B. Abou Hammad, M.S. Abdel-Aziz, A.R. Wassel, Spectroscopic and Antimicrobial Activity of Hybrid Chitosan/Silica Membranes doped with Al2O3 Nanoparticles, Silicon. 11 (2019) 1677–1685. https://doi.org/10.1007/s12633-018-9986-x.

[17] A.M. el Nahrawy, A.M. Bakr, B.A. Hemdan, A.B. Abou Hammad, Identification of Fe3+ co-doped zinc titanate mesostructures using dielectric and antimicrobial activities, International Journal of Environmental Science and Technology. 17 (2020) 4481–4494. https://doi.org/10.1007/s13762-020-02786-x.

[18] A.B. Abou Hammad, A. Elzwawy, A.M. Mansour, M.M. Alam, A.M. Asiri, M.R. Karim, M.M. Rahman, A.M. el Nahrawy, Detection of 3,4-diaminotoluene based on Sr0.3Pb0.7TiO3/CoFe2O4 core/shell nanocomposite: Via an electrochemical approach, New Journal of Chemistry. 44 (2020) 7941–7953. https://doi.org/10.1039/d0nj01074j.

[19] C. Zinge, B. Kandasubramanian, Nanocellulose based biodegradable polymers, European Polymer Journal. 133 (2020) 109758. https://doi.org/10.1016/j.eurpolymj.2020.109758.

[20] M. Suraj Belgaonkar, B. Kandasubramanian, Hyperbranched Polymer-based Nanocomposites: Synthesis, Progress, and Applications, European Polymer Journal. 147 (2021) 110301. https://doi.org/10.1016/j.eurpolymj.2021.110301.

[21] S. Dacrory, A.B. Abou Hammad, A.M. el Nahrawy, H. Abou-Yousef, S. Kamel, Cyanoethyl Cellulose/BaTiO3/GO Flexible Films with Electroconductive Properties, ECS Journal of Solid State Science and Technology. 10 (2021) 083004. https://doi.org/10.1149/2162-8777/ac1c56.

[22] A.M. El Nahrawy, A.B.A.A.B.A. Hammad, A.M. Youssef, A.M. Mansour, A.M. Othman,

Thermal, dielectric and antimicrobial properties of polystyrene-assisted/ITO:Cu nanocomposites, Applied Physics A. 125 (2019) 46. https://doi.org/10.1007/s00339-018-2351-5.

[23] A.M. El Nahrawy, A.A. Haroun, A.B.A. Hammad, M.A. Diab, S. Kamel, Uniformly Embedded Cellulose/Polypyrrole-TiO2 Composite in Sol-Gel Sodium Silicate Nanoparticles: Structural and Dielectric Properties, Silicon. 11 (2019) 1063–1070. https://doi.org/10.1007/s12633-018-9910-4.

[24] A.M. El-Nahrawy, A.I. Ali, A.B. Abou Hammad, A.M. Youssef, Influences of Ag-NPs doping chitosan/calcium silicate nanocomposites for optical and antibacterial activity, International Journal of Biological Macromolecules. 93 (2016) 267–275. https://doi.org/10.1016/j.ijbiomac.2016.08.045.

[25] A.B. Abou Hammad, A.M. Elnahrawy, A.M. Youssef, A.M. Youssef, Sol gel synthesis of hybrid chitosan/calcium aluminosilicate nanocomposite membranes and its application as support for CO2 sensor, International Journal of Biological Macromolecules. 125 (2019) 503–509. https://doi.org/10.1016/j.ijbiomac.2018.12.077.

[26] A.M.S. Mohd Sadiq, B. Arya, C.J.A. Javid Ali, D.N.P. Singh, B.L.S. Sharma, Electrical conductivity and dielectric properties of solid polymer nanocomposite films: Effect of BaTiO3 nanofiller, in: Materials Today: Proceedings, Elsevier, 2019: pp. 476–482. https://doi.org/10.1016/j.matpr.2020.02.623.

[27] Q. Chen, Z. Li, B. Miao, Q. Ma, Thermal, nonlinear, magnetic and faraday rotation properties of sol-gel diamagnetic glass /NaYF4: Fe, Ho3+: Role of magnetic ions, Journal of Alloys and Compounds. 858 (2021) 157631. https://doi.org/10.1016/j.jallcom.2020.157631.

[28] C.P. Hofmann, Diamagnetic and paramagnetic phases in low-energy quantum chromodynamics, Physics Letters B. 818 (2021) 136384. https://doi.org/10.1016/j.physletb.2021.136384.

[29] J. Chen, N.J. Gong, K.T. Chaim, M.C.G. Otaduy, C. Liu, Decompose quantitative susceptibility mapping (QSM) to sub-voxel diamagnetic and paramagnetic components based on gradient-echo MRI data, NeuroImage. 242 (2021) 118477. https://doi.org/10.1016/j.neuroimage.2021.118477.

[30] Y. Guo, J. Zhu, H. Li, Study on structure, magnetic and dielectric properties of li-Zn ferrite with low ferromagnetic resonance line-width and high saturation magnetization synthesized at low temperature by LTCC, Ceramics International. 47 (2021) 9111–9117. https://doi.org/10.1016/j.ceramint.2020.12.034.

[31] A.M. El Nahrawy, B.A. Hemdan, A.M. Mansour, A. Elzwawy, A.B. Abou Hammad, Integrated use of nickel cobalt aluminoferrite/Ni2+ nano-crystallites supported with SiO2 for optomagnetic and biomedical applications, Materials Science and Engineering: B. 274 (2021) 115491. https://doi.org/10.1016/j.mseb.2021.115491.

[32] K.K. Kefeni, T.A.M. Msagati, T.T. Nkambule, B.B. Mamba, Spinel ferrite nanoparticles and nanocomposites for biomedical applications and their toxicity, Materials Science and Engineering: C. 107 (2020) 110314. https://doi.org/10.1016/j.msec.2019.110314.

[33] A.B. Abou Hammad, A.M. Mansour, F. Cao, A.M. El Nahrawy, Effect of Calcination Temperature on the Optical and Magnetic Properties of NiFe 2 O 4 - KFeO 2 Nanocomposite Films Synthesized via WOSW Sol-Gel Route for Opto-Magnetic Applications, ECS Journal of Solid State Science and Technology. 10 (2021) 103016. https://doi.org/10.1149/2162-8777/ac31d2.

[34] A.M. ElNahrawy, A.M. Mansour, H.A. ElAttar, E.M.M. Sakr, A.A. Soliman, A.B.A. Hammad, Impact of Mn-substitution on structural, optical, and magnetic properties evolution of sodium–cobalt ferrite for opto-magnetic applications, Journal of Materials Science: Materials in Electronics. 31 (2020) 6224–6232. https://doi.org/10.1007/s10854-020-03176-2.

[35] L.H. Reddy, J.L. Arias, J. Nicolas, P. Couvreur, Magnetic Nanoparticles: Design and Characterization, Toxicity and Biocompatibility, Pharmaceutical and Biomedical Applications, Chemical Reviews. 112 (2012) 5818–5878. https://doi.org/10.1021/cr300068p.

[36] S. V. Spirou, M. Basini, A. Lascialfari, C. Sangregorio, C. Innocenti, Magnetic hyperthermia and radiation therapy: Radiobiological principles and current practice, Nanomaterials. 8 (2018). https://doi.org/10.3390/nano8060401.

[37] J. Estelrich, M.J. Sánchez-Martín, M.A. Busquets, Nanoparticles in magnetic resonance imaging: From simple to dual

contrast agents, International Journal of Nanomedicine. 10 (2015) 1727–1741. https://doi.org/10.2147/IJN.S76501.
[38] H. Lee, T.-H. Shin, J. Cheon, R. Weissleder, Recent Developments in Magnetic Diagnostic Systems, Chemical Reviews. 115 (2015) 10690–10724. https://doi.org/10.1021/cr500698d.
[39] M.G. Mahfouz, A.A. Galhoum, N.A. Gomaa, S.S. Abdel-Rehem, A.A. Atia, T. Vincent, E. Guibal, Uranium extraction using magnetic nano-based particles of diethylenetriamine-functionalized chitosan: Equilibrium and kinetic studies, Chemical Engineering Journal. 262 (2015) 198–209. https://doi.org/10.1016/j.cej.2014.09.061.
[40] I. Ibrahim, I.O. Ali, T.M. Salama, A.A. Bahgat, M.M. Mohamed, Synthesis of magnetically recyclable spinel ferrite (MFe2O4, M = Zn, Co, Mn) nanocrystals engineered by sol gel-hydrothermal technology: High catalytic performances for nitroarenes reduction, Applied Catalysis B: Environmental. 181 (2016) 389–402. https://doi.org/10.1016/j.apcatb.2015.08.005.
[41] G. Rana, P. Dhiman, A. Kumar, D.-V.N. Vo, G. Sharma, S. Sharma, Mu. Naushad, Recent advances on nickel nano-ferrite: A review on processing techniques, properties and diverse applications, Chemical Engineering Research and Design. 175 (2021) 182–208. https://doi.org/10.1016/j.cherd.2021.08.040.
[42] K.K. Rahangdale, S. Ganguly, Structure, dielectricity and ferroelectricity measurement of new perovskite ceramics (1-x)BaTiO3-xBiMnO3 synthesized by solid-state reaction, Materials Chemistry and Physics. 260 (2021) 124114. https://doi.org/10.1016/j.matchemphys.2020.124114.
[43] W.-Y. Pan, Y.-C. Tang, Y. Yin, A.-Z. Song, J.-R. Yu, S. Ye, B.-P. Zhang, J.-F. Li, Ferroelectric and photovoltaic properties of (Ba, Ca)(Ti, Sn, Zr)O3 perovskite ceramics, Ceramics International. 47 (2021) 23453–23462. https://doi.org/10.1016/j.ceramint.2021.05.061.
[44] A.M. El Nahrawy, A.B. Abou Hammad, A.M. Mansour, Structural investigation and optical properties of Fe, Al, Si, and Cu–ZnTiO 3 nanocrystals, Physica Scripta. 96 (2021) 115801. https://doi.org/10.1088/1402-4896/ac119e.
[45] A.B. Abou Hammad, A.M. Bakr, M.S. Abdel-Aziz, A.M. El Nahrawy, Exploring the ferroelectric effect of nanocrystalline strontium zinc titanate/Cu: Raman and antimicrobial activity, Journal of Materials Science: Materials in Electronics. 31 (2020) 7850–7861. https://doi.org/10.1007/s10854-020-03323-9.
[46] A.B. Abou Hammad, A.M. Mansour, A.M. el Nahrawy, Ni2+doping effect on potassium barium titanate nanoparticles: Enhancement optical and dielectric properties, Physica Scripta. 96 (2021) 125821. https://doi.org/10.1088/1402-4896/ac25a6.
[47] H. Yang, L. Bai, Y. Lin, F. Wang, T. Wang, Magneto-dielectric laminated Ba(Fe0.5Nb0.5)O3-Bi0.2Y2.8Fe5O12 composites with high dielectric constant and high permeability, Ceramics International. 43 (2017) 2903–2909. https://doi.org/10.1016/j.ceramint.2016.09.155.
[48] M. Kumar, K.L. Yadav, Magnetoelectric characterization of xNi0.75Co0.25Fe2O4–(1−x)BiFeO3 nanocomposites, Journal of Physics and Chemistry of Solids. 68 (2007) 1791–1795. https://doi.org/10.1016/j.jpcs.2007.05.006.
[49] J. Van Suchetelene, Product Properties: A New Application of Composite Materials, Philips Res. Rep. 27 (1972) 28–37.
[50] A. Schönhals, F. Kremer, Theory of Dielectric Relaxation, in: Broadband Dielectric Spectroscopy, Springer Berlin Heidelberg, Berlin, Heidelberg, 2003: pp. 1–33. https://doi.org/10.1007/978-3-642-56120-7_1.
[51] A.K. Jonscher, Dielectric relaxation in solids, Journal of Physics D: Applied Physics. 32 (1999) R57–R70. https://doi.org/10.1088/0022-3727/32/14/201.
[52] Y. Poplavko, Broadband dielectric spectroscopy, in: F. Kremer, A. Schönhals (Eds.), Dielectric Spectroscopy of Electronic Materials, Elsevier, Berlin, Heidelberg, 2021: pp. 41–73. https://doi.org/10.1016/B978-0-12-823518-8.00001-3.
[53] K. Deshmukh, S. Sankaran, B. Ahamed, K.K. Sadasivuni, K.S.K. Pasha, D. Ponnamma, P.S. Rama Sreekanth, K. Chidambaram, Dielectric Spectroscopy, in: Spectroscopic Methods for Nanomaterials Characterization, Elsevier, 2017: pp. 237–299. https://doi.org/10.1016/B978-0-323-46140-5.00010-8.
[54] A.M. Neagu, L.P. Curecheriu, A. Cazacu, L. Mitoseriu, Impedance analysis and tunability of BaTiO3–chitosan composites: Towards active dielectrics for flexible electronics, Composites Part B: Engineering. 66 (2014)

109–116. https://doi.org/10.1016/j.compositesb.2014.04.020.
[55] R.H. Cole, Theory of Dielectric Constant and Dielectric Loss., Journal of the American Chemical Society. 80 (1958) 5010–5010. https://doi.org/10.1021/ja01551a071.
[56] A. Schönhals, F. Kremer, Broadband Dielectric Measurement Techniques (10-6 Hz to 1012 Hz), in: Broadband Dielectric Spectroscopy, Springer Berlin Heidelberg, 2003: pp. 35–57. https://doi.org/10.1007/978-3-642-56120-7_2.
[57] S. Havriliak, S. Negami, A complex plane analysis of α-dispersions in some polymer systems, Journal of Polymer Science Part C: Polymer Symposia. 14 (2007) 99–117. https://doi.org/10.1002/polc.5070140111.
[58] K.S. Cole, R.H. Cole, Dispersion and absorption in dielectrics I. Alternating current characteristics, The Journal of Chemical Physics. 9 (1941) 341–351. https://doi.org/10.1063/1.1750906.
[59] D.W. Davidson, R.H. Cole, Dielectric relaxation in glycerine [11], The Journal of Chemical Physics. 18 (1950) 1417. https://doi.org/10.1063/1.1747496.
[60] D.W. Davidson, R.H. Cole, Dielectric Relaxation in Glycerol, Propylene Glycol, and n -Propanol, The Journal of Chemical Physics. 19 (1951) 1484–1490. https://doi.org/10.1063/1.1748105.
[61] A. Schönhals, F. Kremer, Analysis of Dielectric Spectra, in: Broadband Dielectric Spectroscopy, Springer Berlin Heidelberg, Berlin, Heidelberg, 2003: pp. 59–98. https://doi.org/10.1007/978-3-642-56120-7_3.
[62] B. Deka, S. Ravi, D. Pamu, Evolution of structural transition, grain growth inhibition and collinear antiferromagnetism in (Bi1-Sm)FeO3 (x = 0 to 0.3) and their effects on dielectric and magnetic properties, Ceramics International. 43 (2017) 16580–16592. https://doi.org/10.1016/j.ceramint.2017.09.046.
[63] F. Tian, Y. Ohki, Electric modulus powerful tool for analyzing dielectric behavior, IEEE Transactions on Dielectrics and Electrical Insulation. 21 (2014) 929–931. https://doi.org/10.1109/TDEI.2014.6832233.
[64] M. Mumtaz, M. Naveed, S. Akhtar, M. Imran, M.N. Khan, Complex Electric Modulus Spectroscopy of (MnFe2O4)x/CuTl-1223 Nanoparticles-Superconductor Composites, Journal of Superconductivity and Novel Magnetism. 31 (2018) 2691–2698. https://doi.org/10.1007/s10948-017-4547-x.
[65] B.H. Venkataraman, K.B.R. Varma, Microstructural, dielectric, impedance and electric modulus studies on vanadium—doped and pure strontium bismuth niobate (SrBi2Nb2O9) ceramics, Journal of Materials Science: Materials in Electronics. 16 (2005) 335–344. https://doi.org/10.1007/s10854-005-1144-8.
[66] A.R. West, M. Andres-Verges, Impedance and Modulus Spectroscopy of ZnO Varistors, Journal of Electroceramics. 1 (1997) 125–132. https://doi.org/10.1023/A:1009906315725.
[67] A. Roy, K. Prasad, A. Prasad, Piezoelectric, impedance, electric modulus and AC conductivity studies on (Bi0.5Na0.5)0.95Ba0.05TiO3 ceramic, Processing and Application of Ceramics. 7 (2013) 81–91. https://doi.org/10.2298/PAC1302081R.
[68] M. Belal Hossen, A.K.M. Akther Hossain, Complex impedance and electric modulus studies of magnetic ceramic Ni0.27Cu0.10Zn0.63Fe2O4, Journal of Advanced Ceramics. 4 (2015) 217–225. https://doi.org/10.1007/s40145-015-0152-2.
[69] J. Valasek, Piezo-Electric and Allied Phenomena in Rochelle Salt, Physical Review. 17 (1921) 475–481. https://doi.org/10.1103/PhysRev.17.475.
[70] M. Ivanov, J. Macutkevic, R. Grigalaitis, J. Banys, General view of ferroelectrics, in: Magnetic, Ferroelectric, and Multiferroic Metal Oxides, Elsevier, 2018: pp. 5–33. https://doi.org/10.1016/B978-0-12-811180-2.00001-3.
[71] C. Zhang, Z. Zhou, Z. Tang, D. Ballo, C. Wang, G. Jian, Effects of scandium oxide on domain structure, dielectric and ferroelectric properties of barium zirconate titanate ceramics, Journal of Alloys and Compounds. 889 (2021) 161622. https://doi.org/10.1016/J.JALLCOM.2021.161622.
[72] X.K. Wei, S. Prokhorenko, B.X. Wang, Z. Liu, Y.J. Xie, Y. Nahas, C.L. Jia, R.E. Dunin-Borkowski, J. Mayer, L. Bellaiche, Z.G. Ye, Ferroelectric phase-transition frustration near a tricritical composition point, Nature Communications. 12 (2021) 5322. https://doi.org/10.1038/s41467-021-25543-1.
[73] R. Yuan, P. V. Balachandran, D. Xue, Y. Zhou, X. Ding, J. Sun, T. Lookman, D. Xue, Role of cadmium on the phase transitions and electrical properties of BaTiO3 ceramics,

Ceramics International. 43 (2017) 1114–1120. https://doi.org/10.1016/j.ceramint.2016.10.049.

[74] F. Wei, L. Zhang, R. Jing, Q. Hu, D.O. Alikin, Y.Y. Shur, J. Zhang, X. Lu, Y. Yan, H. Du, X. Wei, L. Jin, Structure, dielectric, electrostrictive and electrocaloric properties of environmentally friendly Bi-substituted BCZT ferroelectric ceramics, Ceramics International. 47 (2021) 34676–34686. https://doi.org/10.1016/j.ceramint.2021.09.006.

[75] B.D. Cullity, C.D. Graham, Introduction to Magnetic Materials, John Wiley & Sons, Inc., Hoboken, NJ, USA, 2008. https://doi.org/10.1002/9780470386323.

[76] B.D. Plouffe, S.K. Murthy, L.H. Lewis, Fundamentals and application of magnetic particles in cell isolation and enrichment: a review, Reports on Progress in Physics. 78 (2015) 016601. https://doi.org/10.1088/0034-4885/78/1/016601.

[77] Z. Birčáková, F. Onderko, S. Dobák, P. Kollár, J. Füzer, R. Bureš, M. Fáberová, B. Weidenfeller, J. Bednarčík, M. Jakubčin, J. Szabó, M. Dilyová, Eco-friendly soft magnetic composites of iron coated by sintered ferrite via mechanofusion, Journal of Magnetism and Magnetic Materials. 543 (2022) 168627. https://doi.org/10.1016/j.jmmm.2021.168627.

[78] A. Talaat, M.V. Suraj, K. Byerly, A. Wang, Y. Wang, J.K. Lee, P.R. Ohodnicki, Review on soft magnetic metal and inorganic oxide nanocomposites for power applications, Journal of Alloys and Compounds. 870 (2021) 159500. https://doi.org/10.1016/j.jallcom.2021.159500.

[79] A.M. Leary, P.R. Ohodnicki, M.E. McHenry, Soft Magnetic Materials in High-Frequency, High-Power Conversion Applications, JOM. 64 (2012) 772–781. https://doi.org/10.1007/s11837-012-0350-0.

[80] A. Krings, A. Boglietti, A. Cavagnino, S. Sprague, Soft Magnetic Material Status and Trends in Electric Machines, IEEE Transactions on Industrial Electronics. 64 (2017) 2405–2414. https://doi.org/10.1109/TIE.2016.2613844.

[81] V. Šepelák, D. Baabe, D. Mienert, D. Schultze, F. Krumeich, F.J. Litterst, K.D. Becker, Evolution of structure and magnetic properties with annealing temperature in nanoscale high-energy-milled nickel ferrite, Journal of Magnetism and Magnetic Materials. 257 (2003) 377–386. https://doi.org/10.1016/S0304-8853(02)01279-9.

[82] D.H.K. Reddy, Y.-S. Yun, Spinel ferrite magnetic adsorbents: Alternative future materials for water purification?, Coordination Chemistry Reviews. 315 (2016) 90–111. https://doi.org/10.1016/j.ccr.2016.01.012.

[83] L. a Dobrzanski, M. Drak, B. Zieboqicz, Materials with specific magnetic properties, Journal of Achievements in Materials and Manufacturing Engineering. 17 (2006) 37.

[84] A.O. Adeyeye, G. Shimon, Growth and Characterization of Magnetic Thin Film and Nanostructures, in: Handbook of Surface Science, Elsevier B.V., 2015: pp. 1–41. https://doi.org/10.1016/B978-0-444-62634-9.00001-1.

[85] P. Pahuja, R. Sharma, C. Prakash, R.P. Tandon, Synthesis and characterization of Ni0.8Co0.2Fe2O4–Ba0.95Sr0.05TiO3 multiferroic composites, Ceramics International. 39 (2013) 9435–9445. https://doi.org/10.1016/j.ceramint.2013.05.061.

[86] B. Yang, Z. Li, Y. Gao, Y. Lin, C.-W. Nan, Multiferroic properties of Bi3.15Nd0.85Ti3O12–CoFe2O4 bilayer films derived by a sol–gel processing, Journal of Alloys and Compounds. 509 (2011) 4608–4612. https://doi.org/10.1016/j.jallcom.2011.01.124.

[87] M.M. Vopson, Fundamentals of Multiferroic Materials and Their Possible Applications, Critical Reviews in Solid State and Materials Sciences. 40 (2015) 223–250. https://doi.org/10.1080/10408436.2014.992584.